

# Maximum speed of hypervelocity stars ejected from binaries

Thomas M. Tauris<sup>1,2\*</sup>,

<sup>1</sup> Argelander-Institut für Astronomie, Universität Bonn, Auf dem Hügel 71, D-53121 Bonn, Germany

<sup>2</sup> Max-Planck-Institut für Radioastronomie, Auf dem Hügel 69, D-53121 Bonn, Germany

Accepted 2014 November 26; Received 2014 September 5

## ABSTRACT

The recent detection of hypervelocity stars (HVSs) as late-type B-stars and HVS candidate G/K dwarfs raises the important question of their origin. In this Letter, we investigate the maximum possible velocities of such HVSs if they are produced from binaries which are disrupted via an asymmetric supernova explosion. We find that HVSs up to  $\sim 770$  and  $\sim 1280 \text{ km s}^{-1}$  are possible in the Galactic rest frame from this scenario for these two subclasses of HVSs, respectively. We conclude that whereas a binary origin cannot easily explain all of the observed velocities of B-type HVSs (in agreement with their proposed central massive black hole origin) it can indeed account for the far majority (if not all) of the recently detected G/K-dwarf HVS candidates.

**Key words:** stars: kinematics and dynamics — supernovae: general — binaries: close

## 1 INTRODUCTION

In recent years, a large number of hypervelocity star (HVS) candidates have been reported (e.g. Brown et al. 2005, 2006; Edelmann et al. 2005; Hirsch et al. 2005; Brown et al. 2009, 2012, 2014; Tillich et al. 2009; Li et al. 2012; Palladino et al. 2014; Zhong et al. 2014, and references therein). Here we define genuine HVSs only as stars which will escape the gravitational potential of our Galaxy. Depending on the location and direction of motion, this criterion typically corresponds to a stellar velocity in the Galactic rest frame  $> 400 \text{ km s}^{-1}$  (Kenyon et al. 2008). More than 50 stars can thus be classified as HVSs – see Fig. 1 for a subsample.

HVSs can obtain their large velocities<sup>1</sup> from a number of different processes. Hills (1988) predicted the formation of HVSs via tidal disruption of tight binary stars by the central supermassive black hole (SMBH) of the Milky Way. In this process one star is captured by the SMBH while the other is ejected at high speed via the gravitational slingshot mechanism. Also exchange encounters in other dense stellar environments (e.g. Aarseth 1974) between hard binaries and massive stars may cause stars to be ejected and escape our Galaxy (Leonard 1991; Gvaramadze et al. 2009). A competing mechanism for producing HVSs is disruption of close binaries via supernova (SN) explosions (Blaauw 1961; Boersma 1961; Tauris & Takens 1998; Zubovas et al. 2013). As demonstrated in Tauris & Takens (1998), the runaway velocities of both ejected stars can reach large values when asymmetric SNe are considered, i.e. when the newborn neutron star (NS) receives a momentum kick at birth.

The nature of the HVSs spans a wide range of types from OB-

stars, to metal-poor F-stars and G/K dwarfs. While there is evidence from many late-type B HVSs in the halo to originate from the Galactic SMBH (e.g. Brown et al. 2014) other HVSs seem to originate from the Galactic disc (e.g. Heber et al. 2008; Li et al. 2012; Palladino et al. 2014). This calls for a detailed analysis to explain the kinematic origin of, in particular, the latter group.

In this Letter, we investigate the maximum possible ejection velocities of HVSs with different masses originating from disrupted binaries via asymmetric core-collapse SNe. We use Monte Carlo techniques and perform a systematic investigation of the parameter space prior to/during the SN in order to probe the resulting velocities. The effects of SN shell impact on the companion star are included in our calculations. A particular focus is given to late-type B and G/K-dwarf HVSs. In Section 2 we briefly describe our model. Our results are presented in Section 3 and a discussion follows in Section 4. Our conclusions are summarized in Section 5.

## 2 MODELLING THE DYNAMICAL EFFECTS OF SNE

Tauris & Takens (1998) derived analytical formulae to calculate the velocities of stars ejected from binaries in which asymmetric SNe occur. The velocity of the ejected companion star,  $v_2$  depends on: the pre-SN orbital separation,  $r$ ; its mass,  $M_2$ ; the mass of the exploding star,  $M_{\text{He}}$  (in close binaries often a stripped helium star with a mass of  $3 - 5 M_{\odot}$ ); the mass of the stellar compact remnant (for a NS, typically  $M_{\text{NS}} \simeq 1.4 M_{\odot}$ ); the mass and the velocity of the ejected SN shell,  $M_{\text{ejecta}}$  and  $v_{\text{ejecta}}$ , and the resulting impact velocity on the companion star caused by the ejected shell,  $v_{\text{im}}$  (which depends on the explosion energy,  $E_{\text{SN}}$ ); and finally, the kick velocity (magnitude and direction) imparted on the newborn NS,  $\vec{w}$ .

\* E-mail: tauris@astro.uni-bonn.de

<sup>1</sup> Here we do not distinguish velocity from speed (magnitude of velocity).

## 2 Tauris

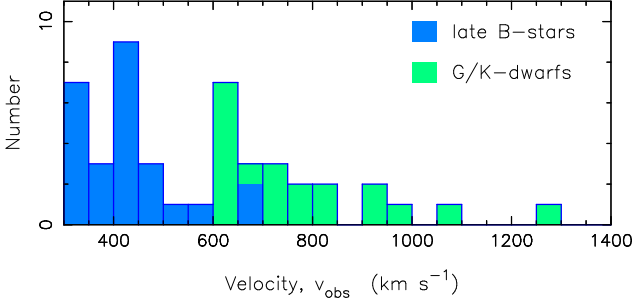


**Figure 1.** Velocity distribution of late B-type HVSS (Brown et al. 2014) and G/K-dwarf HVS candidates (Palladino et al. 2014). The B-star velocities are only based on 1D radial velocities (with typical uncertainties of  $\sigma = \pm 10 \text{ km s}^{-1}$ ). The G/K dwarfs are selected on high proper-motion measurements ( $\sigma = \pm 100 \text{ km s}^{-1}$ ) and may suffer from distance errors. All velocities are given with respect to the Galactic rest frame. The Galactic escape velocity is about  $350 - 400 \text{ km s}^{-1}$  in the halo (Kenyon et al. 2008) and  $\sim 550 \text{ km s}^{-1}$  in the local disc (Smith et al. 2007) – appropriate for many of the observed B-type and G/K-dwarf HVSS, respectively.

The major component affecting the maximum possible ejection velocity of the companion star,  $v_2^{\text{max}}$  is its pre-SN orbital velocity,  $v_{2,\text{orb}}$ . Hence, to produce ejected HVSS it is clear that very close binaries are needed.

The minimum separation between the two stars prior to the SN explosion is assumed to be limited by the Roche-lobe radius of the companion star. The reason for this is that the exploding star itself often fills its Roche lobe (via so-called Case BB Roche-lobe overflow, see e.g. Tauris & van den Heuvel 2006, and references therein). Thus to avoid the onset of a common envelope (e.g. Ivanova et al. 2013), which may lead to a fatal merger event prior to the explosion, we must require that the companion star does not fill its Roche lobe too. Another required constraint in this investigation is that the post-SN trajectory of the NS will not lead to a merger event in an otherwise disrupted system, i.e. if the periastron separation,  $q$  in case of motion along an inbound leg of the hyperbolic orbit ( $\gamma > 0$  and  $\xi > 2$ , in the notation of Tauris & Takens 1998) is smaller than the radius of the companion star,  $R_2$  then the system will likely merge and not produce a HVS.

We applied equations (51–56) of Tauris & Takens (1998) on a large range of binary systems to systematically investigate the maximum possible ejection velocities,  $v_2^{\text{max}}$  by using Monte Carlo simulations. The effects of the SN shell impact are discussed in Appendix A, and a quick sanity check on the applied equations is given in Appendix B.

## 3 RESULTS

In Fig. 2, we have plotted the resulting values of  $v_2$  as a function of kick velocity magnitudes,  $w$  imparted on the NS for one specific set of initial parameters applied to late-type B-star companions with an initial mass of  $3.5 M_{\odot}$  (top) and G/K-dwarf companions with an initial mass of  $0.9 M_{\odot}$  (bottom). In both cases we simulated  $10^6$  explosions using an isotropic kick distribution. All ejection velocities in this Letter ( $v_2$  and  $v_{\text{NS}}$ ) are quoted with respect to the c.m. reference frame of the pre-SN binary. It is interesting to notice that the values of  $v_2^{\text{max}}$  peak when  $w \simeq 1000 - 1200 \text{ km s}^{-1}$  whereas the average values,  $\langle v_2 \rangle$  keep increasing with  $w$  (approaching an asymptotic value as  $w \rightarrow \infty$ , cf. Appendix B).

It is also seen that the values of  $v_2$  for G/K-dwarf stars are generally twice as large as those for the late-type B-stars. This is

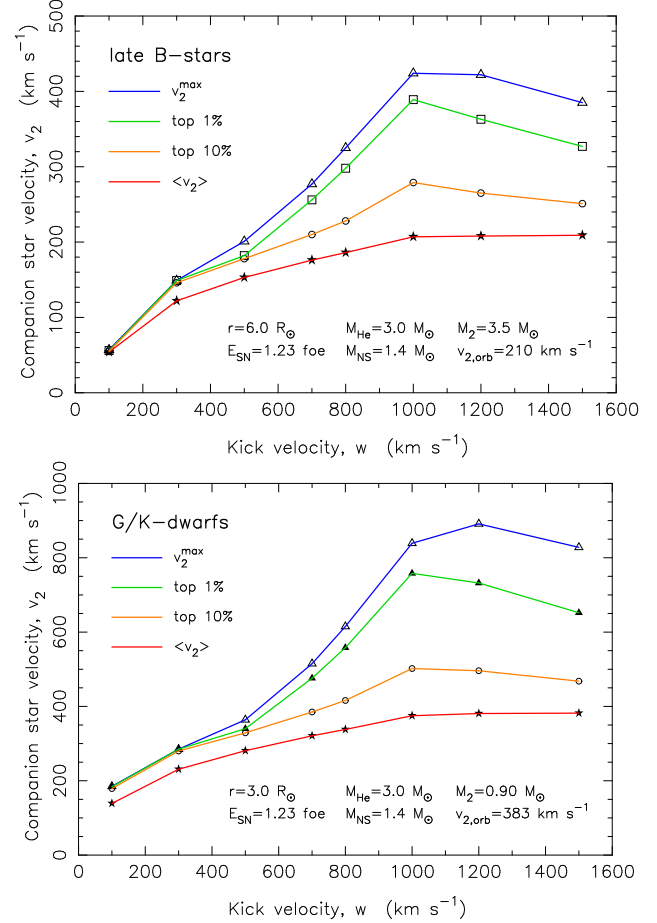


**Figure 2.** Simulated ejection velocities of B-star companions ( $3.5 M_{\odot}$ , top) and G/K-dwarf star companions ( $0.9 M_{\odot}$ , bottom) as a function of the kick velocity magnitude,  $w$  imparted on the NS. In both cases we assumed  $M_{\text{He}} = 3.0 M_{\odot}$ ,  $M_{\text{NS}} = 1.4 M_{\odot}$  and  $E_{\text{SN}} = 1.23 \times 10^{51}$  ergs [note,  $1 \text{ foe} = 10^{51}$  ergs]. The initial (pre-SN) orbital separations were  $6.0$  and  $3.0 R_{\odot}$ , respectively. The four curves in each panel represent the maximum velocities obtained,  $v_2^{\text{max}}$  (blue), the top 1 per cent (green), the top 10 per cent (orange) and the average values,  $\langle v_2 \rangle$  (red), respectively.

mainly caused by the difference in the applied pre-SN orbital separations,  $r$ . The G/K dwarfs are able to remain much closer to the exploding star without filling their Roche lobes ( $r_{\text{min}} \simeq 2.9 R_{\odot}$ , for an exploding star mass of  $M_{\text{He}} = 3.0 M_{\odot}$ ) compared to the more massive, and larger, B-stars ( $r_{\text{min}} \simeq 5.6 R_{\odot}$ , for  $M_{\text{He}} = 3.0 M_{\odot}$ ). Furthermore, the G/K dwarfs have smaller masses,  $M_2$ . As a result of these effects, the G/K dwarfs have larger orbital velocities,  $v_{2,\text{orb}}$  prior to the SN, explaining their larger values of  $v_2$ .

In Fig. 3, we plot the distribution of  $v_2$  and  $v_{\text{NS}}$  for the systems with ejected G/K-dwarf stars plotted in the bottom panel of Fig. 2, and for which  $w = 1000 \text{ km s}^{-1}$ . In this case, as a result of the shell impact, the companion star decreases its mass from  $0.90$  to  $0.846 M_{\odot}$ . About 1.9 per cent of the systems survived as bound binaries, with an average systemic velocity of an impressive  $703 \text{ km s}^{-1}$ , and 3.1 per cent of the systems merged as a result of the SN. The average velocity of the ejected G/K dwarfs is  $\langle v_2 \rangle = 375 \text{ km s}^{-1}$ . However, the entire interval of possible values of  $v_2$  spans between  $87$  and  $839 \text{ km s}^{-1}$  for this particular setup.

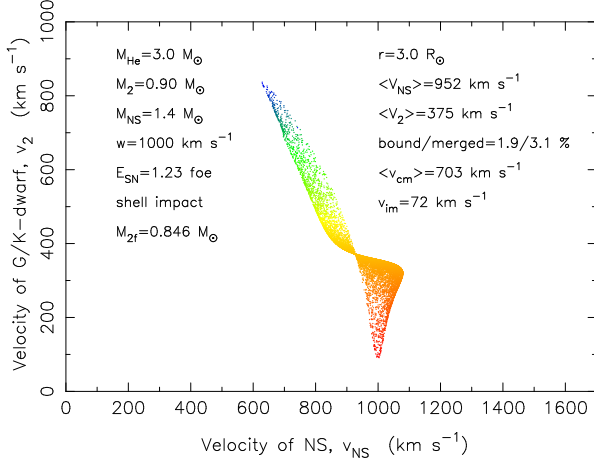


**Figure 3.** Ejection velocities of G/K-dwarf companions,  $v_2$  plotted as a function of the ejection velocities of the newborn NSs,  $v_{\text{NS}}$ . The plot shows  $10^4$  SNe whereas the legend numbers are based on  $10^6$  SNe. The plot was calculated for  $M_2 = 0.9 M_{\odot}$ ,  $w = 1000 \text{ km s}^{-1}$ ,  $M_{\text{He}} = 3.0 M_{\odot}$ ,  $M_{\text{NS}} = 1.4 M_{\odot}$ ,  $E_{\text{SN}} = 1.23 \times 10^{51}$  ergs and  $r = 3.0 R_{\odot}$ .

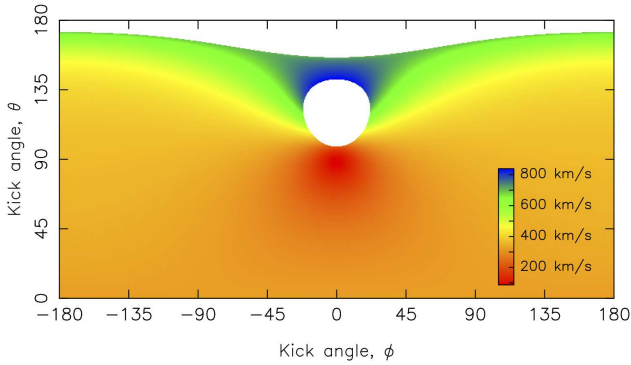


**Figure 4.** Ejection velocities of G/K-dwarf companions plotted as a function of the kick direction angles,  $\theta$  and  $\phi$ . The colours represent the resulting ejection velocities,  $v_2$  varying between  $87 \text{ km s}^{-1}$  (red) and  $839 \text{ km s}^{-1}$  (blue). The plot was calculated for the same initial parameters as in Fig. 3.

### 3.1 Dependence on kick direction

In Fig. 4, we show that the value of  $v_2$  is highly dependent on the direction of the kick imparted on the NS. The white area in the middle corresponds to cases where the newborn NS is shot into the companion star and the system is assumed to merge. For highly retrograde kick directions ( $\theta \rightarrow 180^\circ$ ) the systems remain bound, hence the white area at the top of the plot (the shape of which depends on  $r$  and  $w$ ). The SN-induced HVSS with the largest values of  $v_2$  are ejected close to the plane of the pre-SN binary ( $\phi = 0$ ), causing their spin axis to be almost perpendicular to their velocity vector. While the kick angle  $\phi$  is chosen randomly, the polar kick angle,  $\theta$  is weighted by  $\sin \theta$  in order to obtain an isotropic kick direction (see fig. 1 in Tauris & Takens 1998).

### 3.2 Dependence on pre-SN parameters

As already hinted, besides the kick  $\vec{w}$ , the value of  $v_2$  also depends on pre-SN parameters, in particular the pre-SN orbital separation,  $r$  and the mass of the exploding star,  $M_{\text{He}}$  (see also Eq. B3). This is demonstrated in Fig. 5. The value of  $v_2$  decreases both with increasing values of  $r$  and decreasing values of  $M_{\text{He}}$ . On the other

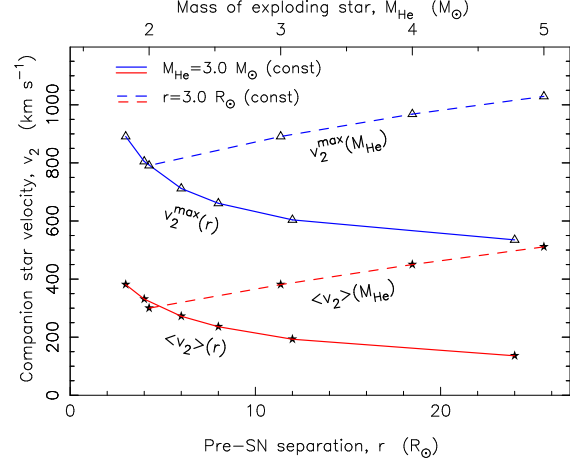


**Figure 5.** Simulated ejection velocities of G/K-dwarf star companions ( $M_2 = 0.9 M_{\odot}$ ) as a function of the pre-SN orbital separation,  $r$  (solid lines) and mass of the exploding star,  $M_{\text{He}}$  (dashed lines). Here we assumed  $w = 1200 \text{ km s}^{-1}$ ,  $E_{\text{SN}} = 1.23 \times 10^{51}$  ergs and  $M_{\text{NS}} = 1.4 M_{\odot}$ . The blue and red lines represent  $v_2^{\text{max}}$  and  $\langle v_2 \rangle$ , respectively.

hand, the dependence of  $v_2$  on the explosion energy,  $E_{\text{SN}}$  is quite weak. For example, using a constant  $w = 1200 \text{ km s}^{-1}$  and increasing the value of  $E_{\text{SN}}$  from 1.23 to 8 foe, only causes  $v_2^{\text{max}}$  to increase by  $\sim 6$  per cent from  $891$  to  $943 \text{ km s}^{-1}$ . The reason for this is that  $v_{2,\text{orb}}^2 \gg v_{\text{im}}^2$  despite the increase in  $E_{\text{SN}}$ .

We emphasize that our aim here is solely to calculate  $v_2^{\text{max}}$ . The general values of  $v_2$  are expected to be much smaller. Although a detailed population synthesis is beyond the scope of this Letter, we made a simple test and found  $\langle v_2 \rangle = 168 \text{ km s}^{-1}$ , if we choose  $r$  randomly between 3 and  $30 R_{\odot}$ , and only apply  $w = 450 \text{ km s}^{-1}$ .

## 4 DISCUSSIONS

We have investigated the maximum runaway velocities of SN-induced HVSS. However, one must bear in mind to add the Galactic rotational velocity (typically of the order of  $v_{\text{Gal}}^{\text{rot}} \simeq \pm 230 \text{ km s}^{-1}$ ) at the birth location of the binary system. Hence, in the Galactic rest frame we obtain  $v_{2,\text{grf}}^{\text{max}} \simeq v_2^{\text{max}} + 230 \text{ km s}^{-1}$ .

### 4.1 B-type HVSS

From our simulations we find that only under the most extreme favourable conditions (with respect to  $r$ ,  $w$ ,  $\theta$ ,  $\phi$ ,  $M_{\text{He}}$  and  $E_{\text{SN}}$ ) is it possible for a late-type B-star ( $\sim 3.5 M_{\odot}$ ) to achieve  $v_2^{\text{max}}$  up to  $\sim 540 \text{ km s}^{-1}$  (in those particular cases  $v_{\text{im}} = 110 \text{ km s}^{-1}$  and the final post-ablation stellar mass is  $\sim 3.24 M_{\odot}$ ). This value implies that  $v_{2,\text{grf}}^{\text{max}} \sim 770 \text{ km s}^{-1}$ . Therefore, any observed B-type HVS which does not exceed this velocity at its origin, and whose trajectory does not point to the central SMBH, could potentially be the result of a disrupted binary. However, we caution that the effect of adding  $v_{\text{Gal}}^{\text{rot}}$  is less important for the HVSS high in the halo and also note that these stars lose some of their kinetic energy along the trajectory to their current location.

Finally, we have investigated disrupted binaries with early, massive B-star companions ( $10 M_{\odot}$ ). Here we find  $v_2^{\text{max}} \sim 320 \text{ km s}^{-1}$ , corresponding to  $v_{2,\text{grf}}^{\text{max}} \sim 550 \text{ km s}^{-1}$ , a significantly lower value compared to the late-type B-stars.

## 4.2 G/K-dwarf HVS candidates

We can reproduce G/K-dwarf HVSs with runaway velocities up to  $v_2^{\max} \simeq 1050 \text{ km s}^{-1}$  (in those extreme cases  $v_{\text{im}} = 195 \text{ km s}^{-1}$ , and the final post-ablation stellar mass is  $\sim 0.71 M_{\odot}$  for a pre-SN mass of  $0.90 M_{\odot}$ ). Hence, in the Galactic rest frame  $v_{2,\text{grf}}^{\max} \sim 1280 \text{ km s}^{-1}$ . Such high velocities can certainly explain many, if not all, of the recently discovered G/K-dwarf HVS candidates (Palladino et al. 2014). Interestingly enough, these HVSs do not seem to originate from the centre of our Milky Way, bringing further support for a disrupted binary scenario as to their origin.

## 4.3 Kick velocities of newborn NSs

In this work the aim has been to calculate the maximum possible runaway velocities for HVSs ejected from disrupted binaries via asymmetric SNe. The magnitude of the kick,  $w$  has been treated as a free parameter (besides the assumption of isotropy in the kick direction) and we find peak values of  $v_2^{\max}$  for  $w = 1000 - 1200 \text{ km s}^{-1}$ . An important question, however, is if such large kicks are realistic? Although the average kick velocities seem to be of the order  $400 - 500 \text{ km s}^{-1}$  (inferred from studies of proper motions of young radio pulsars, Lyne & Lorimer 1994; Hobbs et al. 2005) there are NSs which have received significantly larger kicks. These include the radio pulsars B2011+38 and B2224+65 which (depending on their precise distances) both have 2D velocities exceeding  $1500 \text{ km s}^{-1}$  (Hobbs et al. 2005). The latter pulsar is observed with a bow shock (the ‘‘guitar nebula’’) which confirms that it is moving with a large velocity (Cordes et al. 1993). Another supersonic runaway pulsar with a velocity in excess of  $1000 \text{ km s}^{-1}$  is IGR J11014–6103 (Tomsick et al. 2012; Pavan et al. 2014). Finally, B1508+55 has a fairly precise measured velocity of  $\sim 1100 \pm 100 \text{ km s}^{-1}$  based on VLBA measurements of its proper motion and parallax (Chatterjee et al. 2005).

Further evidence for large kicks can be found from combining simulations of the dynamical effects of SNe with future observations of X-ray binaries with large systemic velocities, following the recipe outlined by Tauris et al. (1999). Given the above-mentioned evidence for large kicks we therefore predict the existence of low-mass X-ray binaries (and binary millisecond pulsars) with peculiar systemic velocities in excess of  $700 \text{ km s}^{-1}$ , cf. Section 3.

Theoretical simulations of SNe (see Janka 2012, for a review) can also account for kicks in excess of  $1000 \text{ km s}^{-1}$  (e.g. Scheck et al. 2006; Wongwathanarat et al. 2013). Hence, our HVS simulations presented in this Letter are based on a solid foundation of evidence for the possibility of large kicks.

## 5 SUMMARY

We have performed systematic Monte Carlo simulations to investigate the maximum possible runaway velocities of HVSs ejected from disrupted binaries via asymmetric SNe. For companion stars with initial masses of  $0.90$ ,  $3.50$  and  $10 M_{\odot}$  we find  $v_{2,\text{grf}}^{\max} = 1280$ ,  $770$  and  $550 \text{ km s}^{-1}$ , respectively. While a significant fraction of late B-type HVS have been shown in the literature to originate from the central SMBH (Brown et al. 2014), we have presented evidence that, in particular, the majority (if not all) of the presently observed G/K-dwarf HVS candidates could very well originate from a binary disruption scenario. However, we caution that a more robust conclusion on the rates and the distribution of  $v_{2,\text{grf}}$  requires detailed population synthesis studies.

Finally, we note that a firm identification of a HVS being ejected from a binary via a SN is still missing, although a candidate (HD 271791) has been proposed by Przybilla et al. (2008); however, see also the interpretation of Gvaramadze (2009).

## ACKNOWLEDGEMENTS

TMT cordially thanks Warren Brown and Pablo Marchant for comments and also acknowledges the receipt of DFG grant TA 964/1-1.

## REFERENCES

- Aarseth S. J., 1974, *A&A*, 35, 237  
 Blaauw A., 1961, *Bull. Astron. Inst. Netherlands*, 15, 265  
 Boersma J., 1961, *Bull. Astron. Inst. Netherlands*, 15, 291  
 Brown W. R., Geller M. J., Kenyon S. J., 2009, *ApJ*, 690, 1639  
 Brown W. R., Geller M. J., Kenyon S. J., 2012, *ApJ*, 751, 55  
 Brown W. R., Geller M. J., Kenyon S. J., 2014, *ApJ*, 787, 89  
 Brown W. R., Geller M. J., Kenyon S. J., Kurtz M. J., 2005, *ApJ*, 622, L33  
 Brown W. R., Geller M. J., Kenyon S. J., Kurtz M. J., 2006, *ApJ*, 640, L35  
 Chatterjee S., et al., 2005, *ApJ*, 630, L61  
 Cheng A., 1974, *Ap&SS*, 31, 49  
 Cordes J. M., Romani R. W., Lundgren S. C., 1993, *Nature*, 362, 133  
 Edelmann H., Napiwotzki R., Heber U., Christlieb N., Reimers D., 2005, *ApJ*, 634, L181  
 Gvaramadze V. V., 2009, *MNRAS*, 395, L85  
 Gvaramadze V. V., Gualandris A., Portegies Zwart S., 2009, *MNRAS*, 396, 570  
 Heber U., Edelmann H., Napiwotzki R., Altmann M., Scholz R.-D., 2008, *A&A*, 483, L21  
 Hills J. G., 1988, *Nature*, 331, 687  
 Hirai R., Sawai H., Yamada S., 2014, *ApJ*, 792, 66  
 Hirsch H. A., Heber U., O’Toole S. J., Bresolin F., 2005, *A&A*, 444, L61  
 Hobbs G., Lorimer D. R., Lyne A. G., Kramer M., 2005, *MNRAS*, 360, 974  
 Ivanova N., et al., 2013, *A&A Rev.*, 21, 59  
 Janka H.-T., 2012, *Annual Review of Nuclear and Particle Science*, 62, 407  
 Kenyon S. J., Bromley B. C., Geller M. J., Brown W. R., 2008, *ApJ*, 680, 312  
 Leonard P. J. T., 1991, *AJ*, 101, 562  
 Li Y., Luo A., Zhao G., Lu Y., Ren J., Zuo F., 2012, *ApJ*, 744, L24  
 Liu Z. W., Pakmor R., Röpke F. K., Edelmann P., Wang B., Kromer M., Hillebrandt W., Han Z. W., 2012, *A&A*, 548, A2  
 Lyne A. G., Lorimer D. R., 1994, *Nature*, 369, 127  
 Marietta E., Burrows A., Fryxell B., 2000, *ApJS*, 128, 615  
 Nomoto K., Thielemann F.-K., Yokoi K., 1984, *ApJ*, 286, 644  
 Pakmor R., Röpke F. K., Weiss A., Hillebrandt W., 2008, *A&A*, 489, 943  
 Palladino L. E., Schlesinger K. J., Holley-Bockelmann K., Allende Prieto C., Beers T. C., Lee Y. S., Schneider D. P., 2014, *ApJ*, 780, 7  
 Pan K.-C., Ricker P. M., Taam R. E., 2012, *ApJ*, 750, 151  
 Pavan L., et al., 2014, *A&A*, 562, A122  
 Przybilla N., Nieva M. F., Heber U., Butler K., 2008, *ApJ*, 684, L103  
 Scheck L., Kifonidis K., Janka H.-T., Müller E., 2006, *A&A*, 457, 963  
 Smith M. C., Ruchti G. R., Helmi A., Wyse R. F. G., et al. 2007, *MNRAS*, 379, 755  
 Tauris T. M., Fender R. P., van den Heuvel E. P. J., Johnston H. M., Wu K., 1999, *MNRAS*, 310, 1165  
 Tauris T. M., Takens R. J., 1998, *A&A*, 330, 1047  
 Tauris T. M., van den Heuvel E. P. J., 2006, *Formation and evolution of compact stellar X-ray sources*. Cambridge University Press, pp 623–665  
 Tillich A., Przybilla N., Scholz R.-D., Heber U., 2009, *A&A*, 507, L37  
 Tomsick J. A., Bodaghee A., Rodríguez J., Chaty S., Camilo F., Fornasini F., Rahoui F., 2012, *ApJ*, 750, L39  
 Wheeler J. C., Lecar M., McKee C. F., 1975, *ApJ*, 200, 145

Wongwathanarat A., Janka H.-T., Müller E., 2013, A&A, 552, A126  
 Zhong J., et al., 2014, ApJ, 789, L2  
 Zubovas K., Wynn G., Gualandris A., 2013, ApJ, 771, 118

## APPENDIX A: THE SUPERNOVA SHELL IMPACT

The formulae of Tauris & Takens (1998) include the impact of the SN shell on the companion star. This effect is significant and must be included when probing the maximum possible ejection velocities since these arise from the tightest pre-SN systems in which the companion star is relatively close to the exploding star (and hence the cross-section for absorbing momentum of the SN ejecta is relatively high). To model the SN shell impact we adopt a modified version of the analytical formulae of Wheeler et al. (1975), following the implementation in Tauris & Takens (1998). While there are several studies published on the shell impact on the companion star in single-degenerate Type Ia SNe, no systematic studies are yet available on similar effects caused by core-collapse SNe (Type Ib/c SNe)<sup>2</sup>. Therefore, we use a new calibration based on more recent multidimensional hydrodynamical simulations of the impact of the ejected shell in single-degenerate Type Ia SNe systems (cf. Marietta et al. 2000; Pakmor et al. 2008; Pan et al. 2012; Liu et al. 2012).

In Figure A1 we show our calibrated fits (dashed lines) given by a slight rewriting of Wheeler et al. (1975):

$$v_{\text{im}} = 0.20 v_{\text{ejecta}} (R_2/2r)^2 (M_{\text{ejecta}}/M_2) x_{\text{crit}}^2 \times \frac{1 + \ln(2 v_{\text{ejecta}}/v_{\text{esc}})}{1 - F^*}, \quad (\text{A1})$$

where  $R_2$  is the radius of the companion star,  $v_{\text{esc}} = \sqrt{2GM_2(x_{\text{crit}})/R} x_{\text{crit}}$  is the surface escape velocity of the companion star (typically,  $800 - 1000 \text{ km s}^{-1}$ ), and the parameter  $x_{\text{crit}}$  is a critical fraction of the radius outside of which a total mass fraction,  $F_{\text{strip}}$  is stripped and inside of which a certain fraction,  $F_{\text{ablated}}$  is ablated. The latter parameters are found from fitted functions to the tabulated values of Wheeler et al. (1975). After the SN shell impact, the new mass of the companion star is given by:  $M_{2f} = M_2(1 - F^*)$ , where we have adopted  $F^* = (F_{\text{strip}} + F_{\text{ablate}})^{1.3}$ . Finally, the average ejecta velocity,  $v_{\text{ejecta}}$  (typically,  $8000 - 10000 \text{ km s}^{-1}$ ) is simply estimated from  $(2 E_{\text{SN}}/M_{\text{ejecta}})^{0.5}$ , where  $E_{\text{SN}}$  is the explosion energy of the SN (although this expression is probably an overestimate by about 10 per cent compared to the results from hydrodynamical studies of SNe, cf. Marietta et al. 2000).

Strictly speaking,  $v_{\text{im}}$  is an *effective* velocity assuming an instant addition of incident shell momentum (stripping) and subsequent momentum resulting from mass loss due to ablation of stellar material from the surface layers heated by the passing shock wave. Although in a close binary the incident energy of the SN debris may exceed the binding energy of the companion star by a few orders of magnitude, this energy is deposited in the outer layers of the star whereby a main-sequence companion star can easily survive such an impact (Cheng 1974; Wheeler et al. 1975).

## APPENDIX B: A SANITY CHECK ON THE EQUATIONS

A quick sanity check on our applied equations (51–56) of Tauris & Takens (1998) is made via their equations (13) and (44–47), and reveals the results for the limiting cases with either no

<sup>2</sup> Although we are aware of work in progress (Z.-W. Liu et al.). Recently, Hirai et al. (2014) presented a novel case with core-collapse SN ejecta interacting with a  $10 M_{\odot}$  giant star companion. However, such a wide orbit (and such a massive companion star) is not suitable for our purposes here.

## 6 Tauris

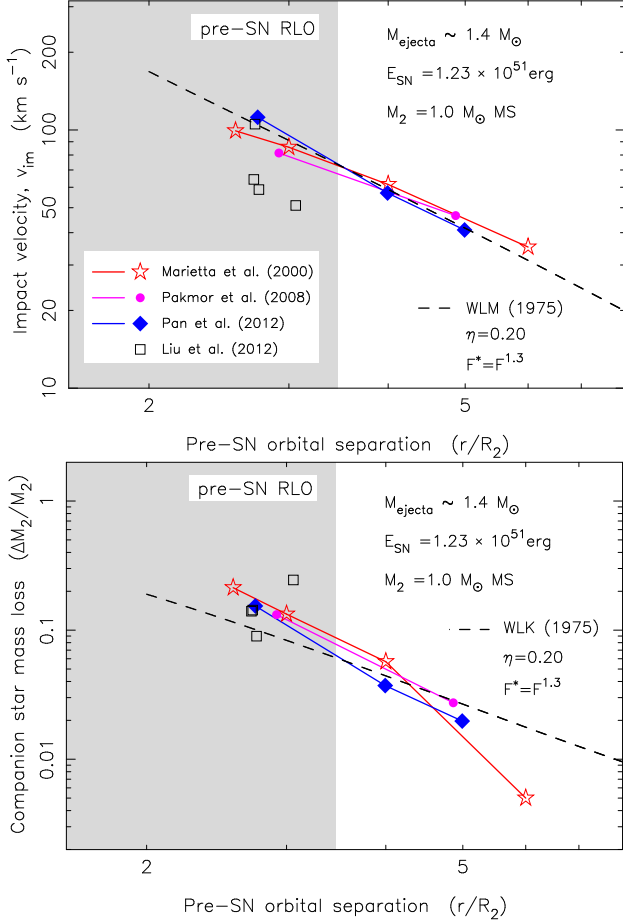


**Figure A1.** Estimates of impact velocity,  $v_{\text{im}}$  (top) and fractional mass loss from the companion star,  $F = \Delta M_2/M_2$  (bottom) as a function of pre-SN orbital separation in units of the companion star radius ( $r/R_2$ ). Our analytical formulae (dashed lines) result from a modified prescription of Wheeler et al. (1975) calibrated on a  $1.0 M_{\odot}$  main sequence star companion. The various symbols show results based on hydrodynamical simulations of  $0.74 - 1.22 M_{\odot}$  companion stars. These calculations were based on Type Ia SNe and thus the ejecta mass,  $M_{\text{ejecta}} \simeq 1.4 M_{\odot}$  (total disruption of a Chandrasekhar-mass white dwarf). The explosion energy is in all cases assumed to be  $1.23 \times 10^{51}$  ergs (model W7 of Nomoto et al. 1984). The shell effects are strongly decreasing with increasing pre-SN orbital separation. The grey-shaded zone corresponds to systems where a  $1.0 M_{\odot}$  companion star (the pre-SN donor star) overfills its Roche lobe in a binary with a  $1.4 M_{\odot}$  accretor (as in a pre-SN Ia binary).

remnant mass (as in the case of SNe Ia) or an infinite high kick velocity:

$$\lim_{M_{\text{NS}} \rightarrow 0} v_2 = \sqrt{v_{2,\text{orb}}^2 + v_{\text{im}}^2}, \quad (\text{B1})$$

$$\lim_{w \rightarrow \infty} v_2 = \sqrt{v_{2,\text{orb}}^2 + v_{\text{im}}^2} \quad \wedge \quad \lim_{w \rightarrow \infty} v_{\text{NS}} = w, \quad (\text{B2})$$

where  $v_2$  is the ejection velocity of the companion star and  $v_{\text{NS}}$  is the ejection velocity of the newborn NS (both in the c.m. reference frame of the pre-SN binary). As discussed in Section 3, in tight pre-SN systems ( $r \rightarrow 0$ ) we have  $v_{2,\text{orb}}^2 \gg v_{\text{im}}^2$  which yields:

$$\lim_{w \rightarrow \infty} v_2 \simeq v_{2,\text{orb}} = M_{\text{He}} \sqrt{G/((M_{\text{He}} + M_2)r)}. \quad (\text{B3})$$

In addition, we have for the case of a purely symmetric SN and neglecting the shell impact (see also Tauris & Takens 1998; Gvaramadze 2009):

$$\lim_{w, v_{\text{im}} \rightarrow 0} v_2 = \sqrt{1 - 2 M_{\text{NS}}(M_{\text{He}} + M_2)/M_{\text{He}}^2} v_{2,\text{orb}}. \quad (\text{B4})$$